

<sup>1</sup> **Submesoscale streamers exchange water on the north  
2 wall of the Gulf Stream**

<sup>3</sup> Jody M. Klymak<sup>1</sup>, R. Kipp Shearman<sup>2</sup>, Jonathan Gula<sup>3</sup>, Craig M. Lee<sup>4</sup>, Eric A. D'Asaro<sup>4</sup>, Leif N.  
<sup>4</sup> Thomas<sup>5</sup>, Ramsey Harcourt<sup>4</sup>, Andrey Shcherbina<sup>4</sup>, Miles A. Sundermeyer<sup>6</sup>, Jeroen Molemaker<sup>7</sup>  
<sup>5</sup> & James C. McWilliams<sup>7</sup>

<sup>6</sup> <sup>1</sup>*University of Victoria, Victoria, British Columbia, Canada*

<sup>7</sup> <sup>2</sup>*Oregon State University, Corvallis, Oregon, USA*

<sup>8</sup> <sup>3</sup>*Laboratoire de Physique des Océans, Université de Bretagne Occidentale, Brest, France*

<sup>9</sup> <sup>4</sup>*Applied Physics Laboratory, University of Washington, Seattle, Washington USA*

<sup>10</sup> <sup>5</sup>*Stanford University, Stanford, California, USA*

<sup>11</sup> <sup>6</sup>*University of Massachusetts Dartmouth, Dartmouth, Massachusetts, USA*

<sup>12</sup> <sup>7</sup>*University of California, Los Angeles, California, USA*

<sup>13</sup> **The Gulf Stream is a major conduit of warm surface water from the tropics to the subpolar**  
<sup>14</sup> **North Atlantic. Its north side has a strong temperature and salinity front that is maintained**  
<sup>15</sup> **for hundreds of kilometers despite considerable energy available for mixing. Large mesoscale**  
<sup>16</sup> ( $> 20$  km) “rings” often pinch off, but like the Gulf Stream they are resistant to lateral  
<sup>17</sup> mixing, and retain their properties for a long time. Here we observe and simulate a sub-  
<sup>18</sup> mesoscale ( $< 20$  km) mechanism by which the Gulf Stream exchanges water with the cold  
<sup>19</sup> subpolar water to the north. A series of “streamers” detrain partially mixed water from the  
<sup>20</sup> Gulf Stream at the crest of meanders. Subpolar water is entrained replacing the partially

21 **mixed water, and helping to resharpen the front. The water mass exchange can account for a**  
22 **northwards flux of salt of  $0.8 - 5 \text{ psu m}^2\text{s}^{-1}$ , which can be cast as an effective local diffusivity**  
23 **of  $O(100 \text{ m}^2\text{s}^{-1})$ . This is similar to bulk-scale flux estimates of  $1.2 \text{ psu m}^2\text{s}^{-1}$  and is enough to**  
24 **supply fresh water to the Gulf Stream as required for the production of 18-degree subtropical**  
25 **mode water.**

26 The Gulf Stream (GS) is the western boundary current of the North Atlantic subtropical  
27 wind-driven circulation. It separates from Cape Hatteras and extends into the interior North At-  
28 lantic, traveling east. As it does so, it loses heat not only to the atmosphere, but also by mixing  
29 with the cold water in the subpolar gyre to the north. It also becomes fresher, an observation that  
30 can only be explained by entrainment of fresh water from the north<sup>1</sup>. As it entrains water, the GS  
31 increases its eastward transport by approximately  $4 - 8 \times 10^6 \text{ m}^3\text{s}^{-1}/100 \text{ km}$  (Johns et. al.  
32 citejohnsetal95). A sharp density front creates thermal wind shear that confines the current to the  
33 upper ocean.

34 The north wall of the GS has a very sharp temperature-salinity front, even along constant-  
35 density surfaces. Salinity decreases by almost 1.5 psu looking north along isopycnals, correspond-  
36 ing to a drop in temperature of  $5^\circ\text{C}$ . The sharpness of this front persists for 100s of kilometers,  
37 despite the fact that mixing along isopycnals is much easier than across them. However, the GS  
38 water has a very high potential vorticity gradient (angular momentum; see methods) that is believed  
39 to act as a barrier to mixing on large scales<sup>2,3</sup>.

40 Despite this barrier and the presence of the sharp front, budgets of properties of the GS

41 indicate that there is significant exchange across the north wall<sup>1</sup>. Entrainment of fresh water is  
42 necessary to create the dynamically important “18-degree water” that fills much of the upper Sar-  
43 gasso Sea. There are large eddies that periodically pinch off the GS and carry warm water to the  
44 north. However, some of these are re-entrained into the GS and do not result in a net exchange.  
45 Instead, tracer budgets across the front appear to be dominated by small-scale processes<sup>4</sup>. To date  
46 some of the best direct evidence for cross-front exchange consists of the trajectories of density-  
47 following floats placed at the north wall<sup>5,6</sup>. These floats were observed to regularly detrain from  
48 the GS, such that of 95 floats, 26 stayed in the GS, 7 were detrained in rings, and 62 were detrained  
49 by mechanisms other than rings<sup>6</sup>. Some floats that detrained were also observed to move upwards  
50 rapidly. Kinematic theories have been examined to explain the detrainment of the floats<sup>7,8</sup>, but  
51 direct observations of the relevant processes have been lacking.

52 Here we present evidence that there is small-scale mixing (<0.5 km) on the northern cyclonic  
53 side of the GS, and that the partially mixed water periodically peels off the GS in thin (5-10 km  
54 wide) “streamers”. In March 2012 we made high-resolution measurements of the north wall of  
55 the GS from 66 W to 60 W (Fig. 1), about 850 km east of where the GS separates from the  
56 North American continental slope. Two research vessels tracked a water-following float placed  
57 in the GS front and programmed to follow the density of the surface mixed layer. The float was  
58 transported downstream with a relatively constant speed of  $1.4 \pm 0.2 \text{ m s}^{-1}$ , in water that became  
59 denser as the surface of the GS cooled. One vessel maintained tight sampling around the float and  
60 deployed an undulating profiler to 200 m, making 10-km cross sections every 10 km downstream.  
61 The second vessel had an undulating profiler making larger 30-km scale sections. Both profilers

62 measured temperature, salinity and pressure, and had approximately 1-km along-track resolution;  
63 both ships also measured ocean currents. Fluorescent dye was deployed near the floats on some  
64 deployments, and measured by the profilers on the ships. By following the float, a focus on the  
65 front was maintained as it curved and meandered to the east.

66 During these observations, the GS had a shallow meander crest at 65 W (Fig. 1b) followed  
67 by a long concave region (63 W) and then another large crest (61 W). Satellite measurements show  
68 the sharp temperature changes across the front, superimposed with thin intermediate-temperature  
69 ( $15\text{-}18^{\circ}\text{C}$ ) streamers detraining to the north at approximately 65 W, 64 W, and at the crest of  
70 the large meander at 61 W. An older streamer that has rolled up can also be seen at 62 W. The  
71 ships passed through the three newer streamers providing the first detailed observations of their  
72 underwater structure.

73 The front consists of density surfaces that slope up towards the north (Fig. 2a-d). The water  
74 along the density surfaces is saltier (and warmer) in the GS, and fresher (and colder) to the north.  
75 The temperature-salinity (T/S) relationship shows the contrast between the two water masses as  
76 two distinct modes (Fig. 3a), except near the surface where the water masses are strongly affected  
77 by the atmosphere. There is a third population between the two larger modes in T/S space that  
78 we identify as the streamers. In the cross-sections, these are the intermediate salinity anomalies  
79 ( $S \approx 36.15$  psu; Fig. 2a-d). Along  $\sigma_{\theta} = 26.25 \text{ kg m}^{-3}$ , these anomalies are horizontally con-  
80 nected, peel off the north wall of the GS, are 5-10 km wide, and stretch for almost 50 km along  
81 the wall (Fig. 3b). The streamers have a strong positive potential vorticity signature. Along the

82 26.25 kg m<sup>-3</sup> isopycnal, the region of high potential vorticity corresponds very well with the par-  
83 tially mixed streamer water (Fig. 2i–l, Fig. 3b ).

84 The streamers remove water from the main GS flow. The velocity contrast across the front  
85 is sharp, with  $> 1 \text{ m s}^{-1}$  drop in 5 km (Fig. 2e–h, Fig. 3b ). The streamers start on the fast side of  
86 the front, moving approximately  $0.25 \text{ m s}^{-1}$  faster than the float (Fig. 2h). Upstream, where they  
87 are detached (Fig. 2e), they are moving almost  $0.5 \text{ m s}^{-1}$  slower than the float. This represents a  
88 considerable detrainment from the GS. A 5-km wide and 150-m deep streamer, detraining with a  
89 relative velocity of  $0.75 \text{ m s}^{-1}$  represents a rate of detrainment of over  $0.5 \times 10^6 \text{ m}^3 \text{s}^{-1}$ .

90 The streamers move up through the water column along isopycnals and the water parcels are  
91 stretched vertically. The streamer in Fig. 2a has risen along isopycnals from 140 m deep (Fig. 2d)  
92 to less than 40 m deep, and titled somewhat as it has done so. The velocity anomaly is about  
93  $0.75 \text{ m s}^{-1}$  over 100 km so we estimate that the streamer is approximately 1.5 days old, implying  
94 vertical velocities of order 50 m/day, similar to rates inferred from large-scale omega-equation  
95 calculations<sup>9</sup>.

96 Concurrently, there is an acceleration of fresh water from the north that is enfolded between  
97 the streamers and the GS, which we will call an “intrusion”. The acceleration of the intrusion is  
98 hard to quantify in the sections above because it is drawn from a large pool of water upstream.  
99 However, a subsequent survey of the north wall (March 14) included a dye release in this reservoir  
100 that was then entrained in an intrusion (Fig. 4a–c). The streamer during this occupation was less  
101 pronounced than the one described above, but was clear for a number of passes through the north

102 wall. The dye cloud was quite spread out, but the data show clear interleaving of the intrusion  
103 water.

104 High-resolution numerical simulations ( $dx \approx 500m$ , see Methods) resolve these features  
105 and also confirm the entrainment of the fresh intrusion (Fig. 4d-i). Seeding the simulation with La-  
106 grangian particles (see methods) allows us to track the evolution of the streamers and the intrusion  
107 as the flow moves downstream. Before the streamer is formed, the water in the intrusion (ma-  
108 genta contours) is near the surface and the streamer water (green contours) is well within the front  
109 (Fig. 4d,g). Downstream (Fig. 4e,h) the fresh water has been subducted to 150 m depth, and the  
110 streamer has been pushed north of the front. Both water masses accelerate with the whole GS be-  
111 tween these two snapshots (Fig. 4f), but the fresh intrusion accelerates more, such that the intrusion  
112 is entrained and the streamer slows and is detrained. As in the observations, the streamer occupies  
113 an intermediate region in T-S space (Fig. 4i, green contour), and originates in the high-vorticity  
114 region of the front.

115 The acceleration of the fresh intrusion relative to the streamer is an important finding of the  
116 model, as the fresh water now forms a new sharp T-S front with the warm salty GS, and the partially  
117 mixed streamer water is carried away from the front. The model further shows that the streamers  
118 are more prominent on the leading edges of meanders, also clearly seen in satellite images (Fig. 1).  
119 There are differences with the observations, however. The data show very distinct T-S signatures  
120 associated with the streamers, whereas the model streamer T/S “mode” is less isolated (Fig. 4i).  
121 The two interleaving water masses are confined to a narrow isopycnal band in the model, with

122 the intrusion being slightly lighter than the streamer, whereas in the observations the temperature-  
123 salinity front cuts across more isopycnals (compare Fig. 2b to Fig. 4h). There is also clear evidence  
124 of strong subduction of the intrusion in the model, reminiscent of intrathermocline eddies<sup>9</sup>.

125 Differences between the data and the model aside, there are two major implications of the  
126 loss of partially mixed water to the north. The first is that it helps explain why the front at the north  
127 wall of the GS remains so sharp. It is not that there is no mixing taking place in both the horizontal  
128 and the vertical, but rather that the mixing product is carried away in the streamers. It is striking  
129 that it is only partially mixed water that is carried away, and not high-salinity GS water (Fig. 3b),  
130 and that this is also high-vorticity water. This implies a dynamical link that we have not seen  
131 explored. Streamers have been observed from surface temperature in satellites and floats<sup>5,7,10,11</sup>,  
132 and this has led to kinematic models in which particles are displaced from streamlines going around  
133 propagating meanders<sup>10,12,13</sup>. The observations here add to these models by showing that it is only  
134 partially mixed water that leaves the GS. This co-incidence indicates to us a role for small-scale  
135 mixing in producing the destabilizing forces that cause this water to detrain from the north wall.  
136 The observations and simulation indicate that the meanders of the GS play an important role in the  
137 formation of the streamers.

138 The second implication is that the streamers are a mechanism that can balance large-scale  
139 budgets that require significant exchange across the GS<sup>1,4</sup>. Such budgets suggest that this region  
140 of the GS loses salinity to the north at a rate of  $1.2 \text{ psu m}^2 \text{s}^{-1}$ <sup>1</sup>. Each streamer transports  $0.2 -$   
141  $0.5 \times 10^6 \text{ m}^3 \text{s}^{-1}$  of water that is  $0.8 - 1 \text{ psu}$  saltier than the water that is entrained. Streamers

<sup>142</sup> appear approximately every 100-300 km, associated with meanders, so an estimate of their average  
<sup>143</sup> transport is  $0.8 - 5 \text{ psu m}^2\text{s}^{-1}$ , bracketing the large-scale estimates. Working against a gradient  
<sup>144</sup> of 1 psu/10 km over 200 m depth, the equivalent lateral diffusivity is  $40 - 250 \text{ m}^2\text{s}^{-1}$ . More  
<sup>145</sup> observations would need to be made to make this transport estimate more robust.

<sup>146</sup> Here we have observed a lateral stirring process along the north wall of the GS. Small-scale  
<sup>147</sup> mixing due to a number of possible processes<sup>?,14</sup> at the north wall temperature-salinity front creates  
<sup>148</sup> an intermediate mass of water that, if it accumulated, would weaken the sharpness of the front.  
<sup>149</sup> However, streamers detrain the partially mixed water, and entrain cold and fresh water toward the  
<sup>150</sup> north wall, resharpening the temperature-salinity front. An alternative possibility is that partially  
<sup>151</sup> mixed water is squeezed by frontogenetic strain, but such squeezing would require this water to  
<sup>152</sup> move downstream. Given the length of the GS, either the intermediate water must accelerate, or  
<sup>153</sup> there is an accumulation somewhere downstream. Given that there is no strong evidence of either  
<sup>154</sup> large-scale acceleration, nor a place where this water mass accumulates, the streamers are a viable  
<sup>155</sup> mechanism that removes this the mixing product.

## <sup>156</sup> 1 Methods

<sup>157</sup> The Lagrangian float was placed in the Gulf Stream front based on a brief cross-stream survey,  
<sup>158</sup> and programmed to match the density of the surface mixed layer (upper 30 m). The float moved  
<sup>159</sup> downstream at a mean speed of  $1.4 \text{ m s}^{-1}$ . The *R/V Knorr* tracked the float and deployed a Chelsea  
<sup>160</sup> Instruments TriAxus that collected temperature, salinity, and pressure (CTD) on a 200-m deep

<sup>161</sup> sawtooth with approximately 1-km lateral spacing in a 10-km box-shaped pattern relative to the  
<sup>162</sup> float (Fig. 1, magenta). *R/V Atlantis* maintained a larger set of cross sections approximately 30 km  
<sup>163</sup> across the front, trying to intercept the float on each front crossing. *R/V Atlantis* was deploying a  
<sup>164</sup> Rolls Royce Marine Moving Vessel Profiler equipped with a CTD that profiled to 200 m approx-  
<sup>165</sup> imately every 1 km. Both ships had a 300 kHz RDI Acoustic Doppler Current Profiler (ADCP)  
<sup>166</sup> collecting currents on 2-m vertical scale averaged every 5 minutes (approximately 1 km lateral  
<sup>167</sup> scale), collected and processed using UHDAS and CODAS (<http://currents.soest.hawaii.edu><sup>15</sup>).  
<sup>168</sup> This data reached about 130 m, and was supplemented at deeper depths with data from 75 kHz  
<sup>169</sup> RDI ADCPs, with 8-m vertical resolution.

<sup>170</sup> Data were interpolated onto depth surfaces by creating a two-dimensional interpolation onto  
<sup>171</sup> a grid via Delauney triangulation. No extrapolation was performed. Data on the  $26.25 \text{ kg m}^{-3}$   
<sup>172</sup> isopycnal were assembled at each grid point by finding the first occurrence of that isopycnal in  
<sup>173</sup> depth.

<sup>174</sup> Potential vorticity is calculated from the three-dimensional grid as

$$q = -\frac{g}{\rho_0} (\nabla \times \mathbf{u} + \mathbf{f}) \cdot \nabla \rho, \quad (1)$$

<sup>175</sup> where  $f$  is the Coriolis frequency,  $g$  the gravitational acceleration. The bracketed term is twice  
<sup>176</sup> the angular velocity, including the planet's rotation, and the gradient of density represents the  
<sup>177</sup> stretching or compression of the water column. In the GS, the potential vorticity is dominated by  
<sup>178</sup> contributions from the vertical density gradient and the cross-stream gradient of the along-stream

179 velocity:

$$q \approx N^2 \left( -\frac{\partial u}{\partial y} + f \right). \quad (2)$$

180 Dye Release. At select times during the float evolutions, fluorescein dye releases (100 kg  
181 per release) were conducted at depth as close as possible to the float. Dye was pumped down a  
182 garden hose to a tow package deployed off the side of the ship, consisting of a CTD and a dye  
183 diffuser. Prior to injection, the dye was mixed with alcohol and ambient sea water to bring it to  
184 within  $0.001 \text{ kg m}^{-3}$  of the float's target density. Initial dimensions of the dye streak were  $\approx 1$   
185 km along-stream,  $\approx 100 \text{ m}$  cross-stream (after wake adjustment), and ranging from 1 - 5 m in the  
186 vertical. The TriAxis system on the *R/V Knorr* tracked the fluorescein from its CTD package.

187 Numerical simulation. The high-resolution realistic simulation of the GS is performed with  
188 the Regional Oceanic Modeling System (ROMS<sup>16</sup>). This simulation has a horizontal resolution of  
189 500m and 50 vertical levels. The model domain spans 1,000 km by 800 km and covers a region  
190 of the GS downstream from its separation from the U.S. continental slope. Boundary conditions  
191 are supplied by a sequence of two lower-resolution simulations that span the entire GS region and  
192 the Atlantic basin, respectively. The simulation is forced by daily winds and diurnally modulated  
193 surface fluxes. The modelling approach is described in detail in Gula et. al<sup>17</sup>.

194 Virtual Lagrangian Particles. The neutrally buoyant Lagrangian (flow-following) particles  
195 were seeded at time 285 and advected both backwards and forwards from this time by the model  
196 velocity fields without additional dispersion from the model's mixing processes<sup>18</sup>. A 4th-order

<sup>197</sup> Runge-Kutta method with a time step  $dt = 1$  s is used to compute particle advection. Velocity and  
<sup>198</sup> tracer fields are interpolated at the positions of the particles using cubic spline interpolation in both  
<sup>199</sup> the horizontal and vertical directions. We use hourly outputs from the simulation to get sufficiently  
<sup>200</sup> frequent and temporally-smooth velocity sampling for accurate parcel advection.

- <sup>202</sup> 1. Joyce, T. M., Thomas, L. N., Dewar, W. K. & Girton, J. B. Eighteen degree water formation  
<sup>203</sup> within the Gulf Stream during CLIMODE. *Deep Sea Res. II* (2013).
- <sup>204</sup> 2. Marshall, J., Shuckburgh, E., Jones, H. & Hill, C. Estimates and implications of surface  
<sup>205</sup> eddy diffusivity in the Southern Ocean derived from tracer transport. *J. Phys. Oceanogr.* **36**,  
<sup>206</sup> 1806–1821 (2006).
- <sup>207</sup> 3. Naveira Garabato, A. C., Ferrari, R. & Polzin, K. L. Eddy stirring in the southern ocean. *J.*  
<sup>208</sup> *Geophys. Res.* **116** (2011).
- <sup>209</sup> 4. Bower, A. S., Rossby, H. T. & Lillibridge, J. L. The Gulf Stream-barrier or blender? *J. Phys.*  
<sup>210</sup> *Oceanogr.* **15**, 24–32 (1985).
- <sup>211</sup> 5. Bower, A. & Rossby, T. Evidence of cross-frontal exchange processes in the Gulf Stream  
<sup>212</sup> based on isopycnal rafos float data. *J. Phys. Oceanogr.* **19**, 1177–1190 (1989).
- <sup>213</sup> 6. Bower, A. S. & Lozier, M. S. A closer look at particle exchange in the Gulf Stream. *J. Phys.*  
<sup>214</sup> *Oceanogr.* **24**, 1399–1418 (1994).
- <sup>215</sup> 7. Flierl, G., Malanotte-Rizzoli, P. & Zabusky, N. Nonlinear waves and coherent vortex structures  
<sup>216</sup> in barotropic  $\beta$ -plane jets. *J. Phys. Oceanogr.* **17**, 1408–1438 (1987).

- 217 8. Stern, M. E. Lateral wave breaking and “shingle” formation in large-scale shear flow. *J. Phys.*
- 218 *Oceanogr.* **15**, 1274–1283 (1985).
- 219 9. Thomas, L. N. & Joyce, T. M. Subduction on the northern and southern flanks of the Gulf
- 220 Stream. *J. Phys. Oceanogr.* **40**, 429–438 (2010).
- 221 10. Lozier, M., Pratt, L., Rogerson, A. & Miller, P. Exchange geometry revealed by float trajectories
- 222 in the Gulf Stream. *J. Phys. Oceanogr.* **27**, 2327–2341 (1997).
- 223 11. Song, T., Rossby, T. & Carter, E. Lagrangian studies of fluid exchange between the Gulf
- 224 Stream and surrounding waters. *J. Phys. Oceanogr.* **25**, 46–63 (1995).
- 225 12. Bower, A. S. A simple kinematic mechanism for mixing fluid parcels across a meandering jet.
- 226 *J. Phys. Oceanogr.* **21**, 173–180 (1991).
- 227 13. Pratt, L. J., Susan Lozier, M. & Beliakova, N. Parcel trajectories in quasigeostrophic jets:
- 228 Neutral modes. *J. Phys. Oceanogr.* **25**, 1451–1466 (1995).
- 229 14. Whitt, D. B. & Thomas, L. N. Near-inertial waves in strongly baroclinic currents. *J. Phys.*
- 230 *Oceanogr.* **43**, 706–725 (2013).
- 231 15. Firing, E., Hummon, J. M. & Chereskin, T. K. Improving the quality and accessibility of
- 232 current profile measurements in the southern ocean. *Oceanography* (2012).
- 233 16. Shchepetkin, A. & McWilliams, J. The regional oceanic modeling system (ROMS): a split-
- 234 explicit, free-surface, topography-following-coordinate oceanic model. *Ocean Modell.* **9**, 347–
- 235 404 (2005).

- <sup>236</sup> 17. Gula, J., Molemaker, M. J. & McWilliams, J. C. Gulf stream dynamics along the southeastern  
<sup>237</sup> us seaboard. *J. Phys. Oceanogr.* **45**, 690–715 (2015).
- <sup>238</sup> 18. Gula, J., Molemaker, M. J. & McWilliams, J. C. Submesoscale cold filaments in the gulf  
<sup>239</sup> stream. *J. Phys. Oceanogr.* **44**, 2617–2643 (2014).

240 List of Figures

251        2     **Cross sections of data collected across the Gulf Stream.**  $Y$  is the cross-stream  
252        distance perpendicular to the path of the float, positive being northwards. The four  
253        columns correspond to the four sections labeled a-d in Fig. 1. Potential density is  
254        contoured in black and  $\sigma_\theta = 26.25 \text{ kg m}^{-3}$  is magenta. Along a constant density  
255        surface salty water is warmer than fresher water, so the GS on the left is warm  
256        and salty. Section a) is the furthest upstream section (65W) and d) is the furthest  
257        downstream (63.75 W) (Fig. 3b). e)-h) downstream velocity calculated relative to  
258        the float's trajectory by removing the float's mean speed of  $u_{\text{float}} = 1.4 \text{ m s}^{-1}$  for  
259        the observation period. Green contours are regions in temperature-salinity space  
260        labeled "streamers" in Fig. 3a. i)-l) Potential vorticity sections (see text); . . . . . 19

261        3     **Streamer properties and distribution in space.** a) Logarithmically scaled his-  
262        togram in temperature-salinity space (colours). The warm-salty GS water is very  
263        distinct from the water to the north, which is cold and fresh. The water near the  
264        surface is heavily modified by the atmosphere. Deeper, there is a class of water  
265        distinct from the GS water and the water to the north, that we label "streamers".  
266        This water is contoured in green in Fig. 2e-l. b) Interpolation of salinity, velocity,  
267        and potential vorticity onto the  $\sigma_\theta = 26.25 \text{ kg m}^{-3}$  isopycnal, plotted geographi-  
268        cally (with a small exaggeration of scale in the north-south direction, and the latter  
269        two fields offset slightly to the south-east). This used data from both ships. The  
270        ship track for the *Atlantis* is plotted in black, and the four cross-sections in Fig. 2  
271        are plotted in magenta. The streamer water is contoured in green. . . . . . . . . . . 20



295 **Acknowledgements** Our thanks to the captains and crews of *R/V Knorr* and *R/V Atlantis*, The AVHRR  
296 Oceans Pathfinder SST data were obtained from the Physical Oceanography Distributed Active Archive Cen-  
297 ter (PO.DAAC) at the NASA Jet Propulsion Laboratory, Pasadena, CA. <http://podaac.jpl.nasa.gov>. Funding  
298 was supplied by Office of Naval Research, Grants XXXXXX

299 **Competing Interests** The authors declare that they have no competing financial interests.

300 **Correspondence** Correspondence and requests for materials should be addressed to Jody M. Klymak. (email:  
301 [jklymak@uvic.ca](mailto:jklymak@uvic.ca)).

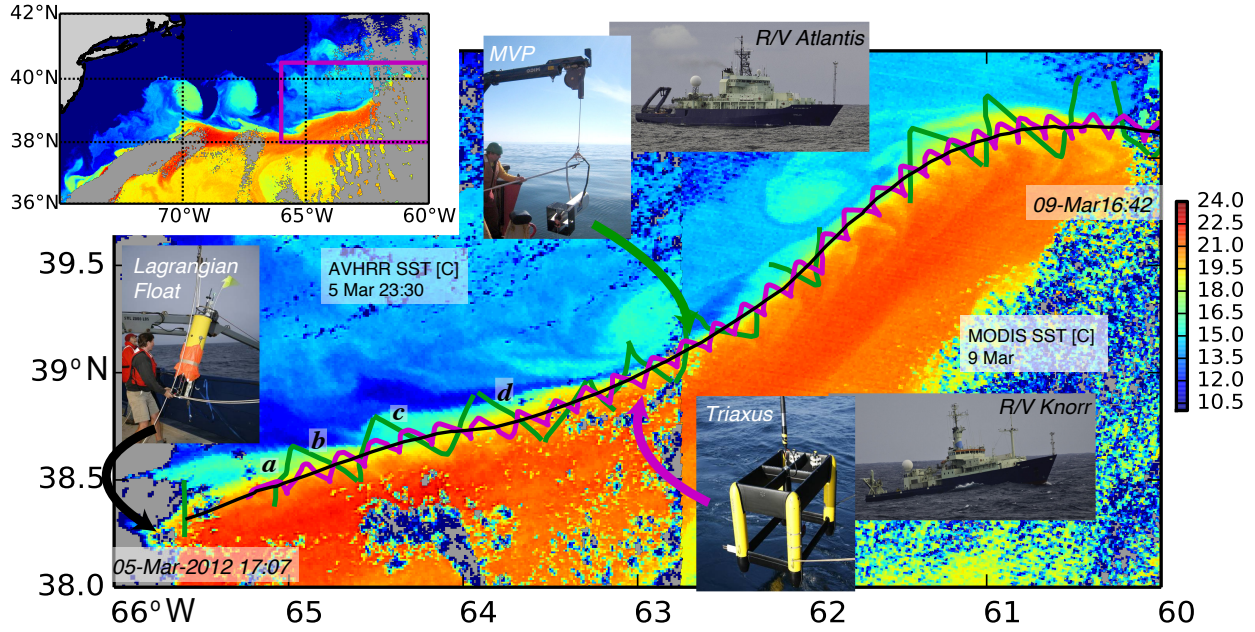


**Figure 1: Experimental design.** Inset: The experiment site on the north wall of the Gulf Stream, between 66 and 60 W, as shown in an AVHRR satellite image of sea surface temperature (SST). Main: Detailed SST image composed from two satellites images. The GS is warm and delineated by a sharp front. There are small sub-mesoscale structures north of the front, which are the focus of this paper. The satellite images are a composite from early in the observation period (AVHRR 6 Mar), and late (MODIS, 9 Mar). A Lagrangian float was deployed in the front (black curve), and the ship tracks bracketed the float's position (green: *R/V Atlantis*, magenta: *R/V Knorr*). *R/V Atlantis* cross-sections labeled a-d are shown in Fig. 2a-d.

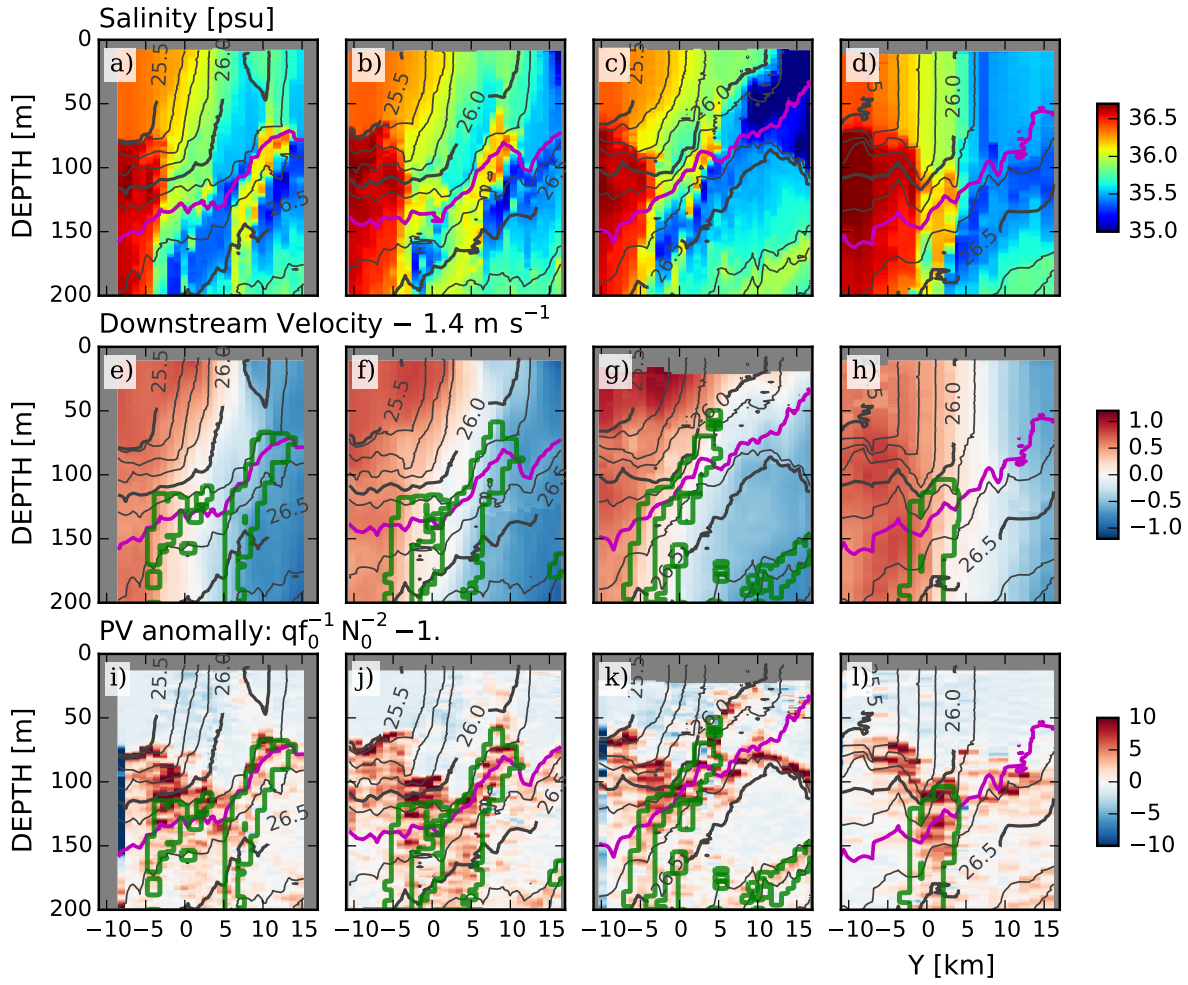


**Figure 2: Cross sections of data collected across the Gulf Stream.**  $Y$  is the cross-stream distance perpendicular to the path of the float, positive being northwards. The four columns correspond to the four sections labeled a-d in Fig. 1. Potential density is contoured in black and  $\sigma_\theta = 26.25 \text{ kg m}^{-3}$  is magenta. Along a constant density surface salty water is warmer than fresher water, so the GS on the left is warm and salty. Section a) is the furthest upstream section (65W) and d) is the furthest downstream (63.75 W) (Fig. 3b). e)–h) downstream velocity calculated relative to the float's trajectory by removing the float's mean speed of  $u_{\text{float}} = 1.4 \text{ m s}^{-1}$  for the observation period. Green contours are regions in temperature-salinity space labeled “streamers” in Fig. 3a. i)–l) Potential vorticity sections (see text);

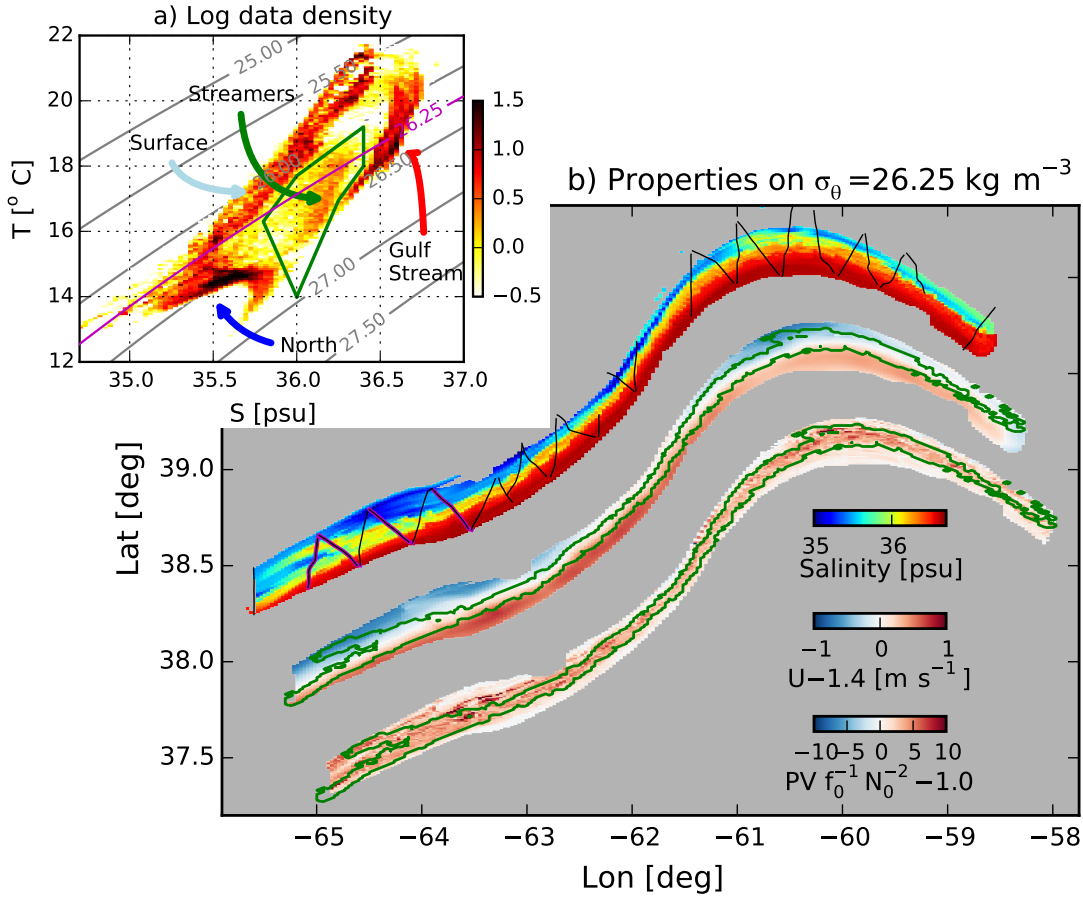


**Figure 3: Streamer properties and distribution in space.** a) Logarithmically scaled histogram in temperature-salinity space (colours). The warm-salty GS water is very distinct from the water to the north, which is cold and fresh. The water near the surface is heavily modified by the atmosphere. Deeper, there is a class of water distinct from the GS water and the water to the north, that we label “streamers”. This water is contoured in green in Fig. 2e-l. b) Interpolation of salinity, velocity, and potential vorticity onto the  $\sigma_\theta = 26.25 \text{ kg m}^{-3}$  isopycnal, plotted geographically (with a small exaggeration of scale in the north-south direction, and the latter two fields offset slightly to the south-east). This used data from both ships. The ship track for the *Atlantis* is plotted in black, and the four cross-sections in Fig. 2 are plotted in magenta. The streamer water is contoured in green.

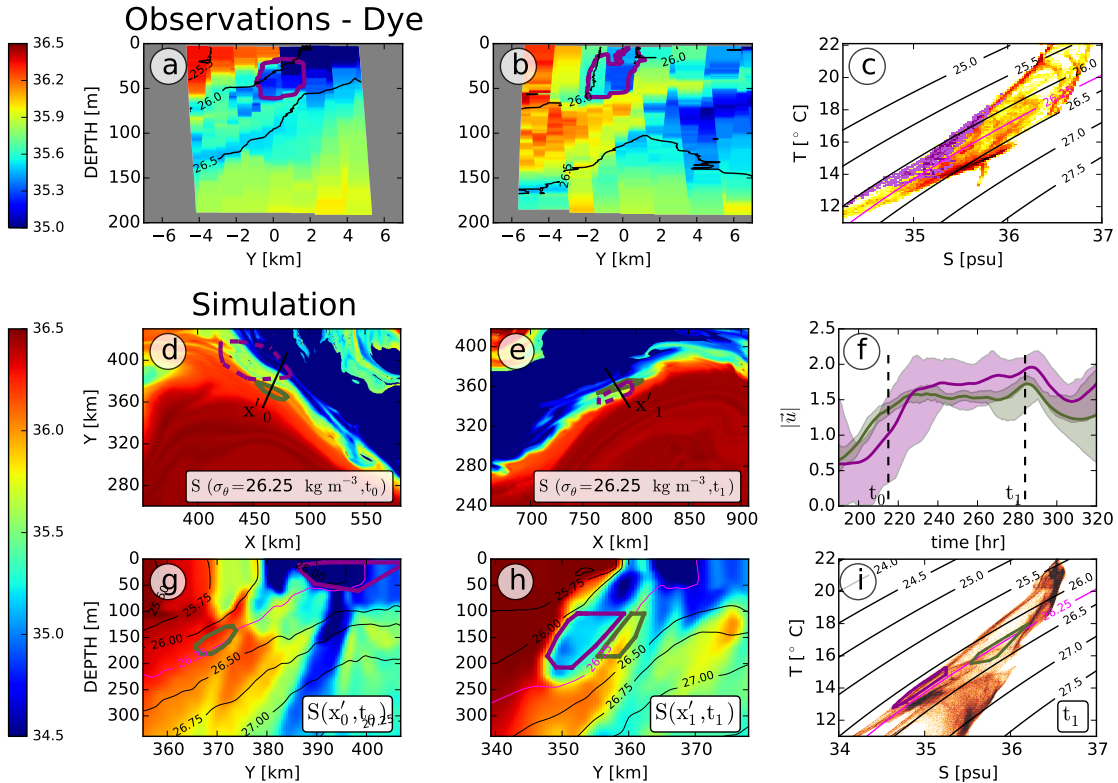


Figure 4: **Evidence for entrainment of intrusions from a dye release and numerical simulation.**

a) Salinity section from an occupation of the GS 14 March. The location of a dye is contoured in magenta. b) Salinity section from downstream. A streamer has enfolded the dye in cold-fresh water between itself and the GS. c) Temperature-salinity diagram for this occupation. The temperature-salinity for the dye is coloured in dark magenta. d) Salinity in the GS on the  $\sigma_\theta = 26.25 \text{ kg m}^{-3}$  isopycnal from a high-resolution numerical simulation at  $t_0$ . The green contours delineate the location of particles seeded downstream in the streamer at time  $t_1 = t_0 + 70\text{h}$  (see panels e and h) and advected *backwards* in time to  $t_0$  showing where the streamer water originated. The dark magenta contour is the location of particles seeded in the fresh intrusion. The straight line shows the location of the salinity cross-section in panel g. e) as panel d, except at  $t_1 = t_0 + 70\text{ h}$ ; this is the time and locations where the two clouds of particles were seeded. g) and h) salinity cross sections for times  $t_0$  and  $t_1$ . The location of the particles is shown in green and dark magenta contours. The  $\sigma_\theta = 26.25 \text{ kg m}^{-3}$  isopycnal is contoured in light magenta. These panels show that the origin of the streamer water was in the GS front, and that the fresh-cold water